Molecular Crystals and Liquid Crystals

ISSN: 1542-1406 (Print) 1563-5287 (Online) Journal homepage: http://www.tandfonline.com/loi/gmcl20

Structural and optical properties of novel nematogens based on DFT and semiempirical method—A comparative picture

Durga P. Ojha

To cite this article: Durga P. Ojha (2016) Structural and optical properties of novel nematogens based on DFT and semiempirical method—A comparative picture, Molecular Crystals and Liquid Crystals, 633:1, 91-99, DOI: 10.1080/15421406.2016.1177888

To link to this article: http://dx.doi.org/10.1080/15421406.2016.1177888

Published online: 24 Aug 2016.

MOLECULAR CRYSTALS AND LIQUID CRYSTALS
2016, VOL. 633, 91–99
http://dx.doi.org/10.1080/15421406.2016.1177888

Taylor & Francis
Taylor & Francis Group

Structural and optical properties of novel nematogens based on DFT and semiempirical method—A comparative picture

Durga P. Ojha

School of Physics, Sambalpur University, Jyoti Vihar, Sambalpur, Odisha, India

ABSTRACT

A comparative picture of structural, and optical properties of nematogens, viz., bis(4-propyloxyphenyl) 1,12-dicarba-closo-dodecaborane-1,12-dicarboxylate (Nematic1), and bis(4-butoxyphenyl) 1,10-dicarba-closo-decaborane-1,10-dicarboxylate (Nematic2) have been studied in ultraviolet (UV) and visible (Vis) regions. The structure of nematogens have been optimized using the Density functional B3LYP with 6–31+G (d) basis set using crystallographic geometry as input. The electronic structure of the molecules has been evaluated using the DFT, and semiempirical methods, namely; CNDO/S (complete neglect of differential overlap/ spectroscopy) and INDO/S (intermediate neglect of differential overlap/ spectroscopy). The HOMO (Highest Occupied Molecular Orbital)/LUMO (Lowest Unoccupied Molecular Orbital) energies, and oscillator strength (f) have also been reported using these methods. The electronic absorption spectra of the molecules have been simulated by employing the DFT method, semiempirical parameterizations. Molecular charge distribution and phase stability of these nematogens have been analyzed based on Mulliken and Loewdin population analysis. It has been observed that Nematic2 molecule shows the much flexibility for electronic transitions over a long wavelength region that leads to high photosensitivity.

KEYWORDS

Optical properties; nematogens; DFT method

Introduction

The technological benefits of the advances in the field of liquid crystals (LCs) is evident by the existence of a variety of consumer products that use these materials in the display devices ranging from simple indicators to sophisticated color laptop computers [1]. The scientific break through in this field is equally impressive, with discoveries of new phases with the different structures and properties [2]. These structures and phases may also lead to unique applications of these materials. The photo-induced phenomena of liquid crystal derivatives, in which the light can be acting as a stimulus and control parameter, have attracted a significant amount of attention because of the promising applications of these molecules in the development of various display and photonic devices, such as erasable optical data storage, and optical switch components. Most of the studies are focused on phase transition temperatures, and optical properties of these photosensitive systems, as these characteristics are critical for their applications in different devices [3].

CONTACT Durga P. Ojha durga_ojha@hotmail.com School of Physics, Sambalpur University, Jyoti Vihar 768019, Sambalpur, Odisha, India.

Color versions of one or more of the figures in the article can be found online at www.tandfonline.com/gmcl.

The systems chosen for the present investigation, i.e., C*loso*-Boranes are characterized by high thermal and oxidative stability due in part to highly delocalized bonding within an σ-framework [4]. Their thermal stability, delocalized bonding, and ease of functionalization have the potential to alter the electronic structure, and therefore response, of the bulk liquid crystalline material to external electric or magnetic field.

Ultraviolet (UV) absorption behavior of LCs is significant, as they maintain the ability to interact with light. Such properties are desirable in the design of new LC materials to achieve high electronic polarizability, low anisotropy, which would result in low birefringence [5], and a high isotropic refractive index [6] for a boron containing LC [7]. The calculation of UV–vis spectra is appealing since a large number of methods have been employed to calculate the absorption wavelength and oscillator strength of electronic transitions. The methods based on Time Dependent Density Functional Theory (TDDFT) applied to small- and middle-sized systems provide rather good accuracy at low computational cost [8]. These methods still remain of rather limited application for establishing realistic molecular models. Hence, the alternate use of semiempirical schemes has an extensive use to analyze absorption behavior. Such approaches allow the calculation of electronic transitions between the ground state, and the different excited states that provides the energies of the corresponding radiations. Subtle changes in the molecular structure of molecules lead to great variations on both physical properties like stability, optical and electronic properties such as absorption behaviour, energy gap, electron affinity, etc.

The present article deals with a comparative picture of structural, and optical properties of Nematic1, and Nematic2 using the semiempirical CNDO/S [9–13], INDO/S [14, 15] schemes, and DFT method. The HOMO/LUMO energies and oscillator strength (*f*) have also been reported using these methods. The general structural parameters of the systems such as bond lengths and bond angles have been taken from the published crystallographic data [16] to construct the electronic structures.

Computational approach

DFT approach

The optical absorption behavior requires the knowledge of molecular orbitals properties, spectral shifts, and appropriate excited states. The main difficulties against reliable theoretical models are concerned with the size of systems, and the presence of strong electron correlation effects. Both properties are difficult to treat in the framework of the quantum-mechanical methods rooted in the Hartree–Fock (HF) theory. The Density functional theory (DFT) is successful to evaluate a variety of ground-state properties with accuracy close to that of post-HF methods [17, 18].

The exchange correlation functional used in the calculation is an important factor that determines the accuracy of TDDFT excitation energies. The use of these hybrid functional yields good accounts of the vertical excitation energies of the excited states with substantial charge transfer character. In this context, The B3LYP (Becke–Lee–Yang–Parr) version of DFT is the combination of Becke's three-parameter non-local hybrid functional of exchange terms [19] with the Lee, Yang, and Parr correlation functional [20]. The basis set of 6–31+G (d) contains a reasonable number of basis set functions that are able to reproduce the experimental data. As a consequence, there is currently a great interest in extending DFT to excited electronic states. The TDDFT approach offers a rigorous route to the calculation of vertical electronic excitation energies and other spectral characteristics [8].

Semiempirical approach

The ground state of a closed-shell system is generally well represented by a single determinantal wavefunction. However, the full CI calculations are required for an accurate representation of excited states. The corresponding calculations of molecules have been made using the CNDO/S, and INDO/S methods. In these two methods, the wavefunctions of the ground, and once electronically excited states of $\pi\pi^*$-type for a molecule have been calculated in the one-configurational approximation. The electronic absorption spectrum has been calculated using the method of CI on the basis of obtained multi-electron wavefunctions of molecules. In the CIS approach, orbitals of the H-F solution have been used to generate all singly excited determinants of the CI expansion. This treatment can be thought as the H-F method for excited states.

It is well-known fact that semiempirical molecular orbital method has always been calibrated using a set of trial functions. In addition to the shortcomings, which result from the inherent structure of the method due to the particular approximations, use of the different set of trial functions may require a reparameterization of the method. The ZINDO [14, 20, 21] has been specifically parameterized to give the theoretical transition energies, and the respective intensities of molecules in the UV range with a given CI expansion of singly excited determinants. The electronic configurations considered here are generated by promoting one electron from the HOMO to the LUMO. Further, the introduction of levels has been performed to test the validity of approach, and it does not change the results significantly. The scaling of the CI space [22] should correct somewhat for the size extensively error of the CI. Furthermore, the results obtained by using a larger CI for smaller systems show little dependence on the CI space. The spectroscopic data were convoluted with Gaussian line shapes as a function of the wavelengths.

Geometries optimizations

The geometries optimizations have been performed using the DFT approach, the hybrid functional B3LYP [20], exchange-correlation functional, and the 6–31+G (d) basis set. The DFT approach was originally developed by Hohenberg and Kohn [20], Kohn and Sham [23, 24] to provide an efficient method of handling the many-electron system. The theory allows us to reduce the problem of an interacting many-electron system to an effective single-electron problem. On the basis of the DFT geometries, the electronic structures, excitation energies, and excited state wavefunctions have been calculated coupled with the configuration interaction (CI) single level of approximation including all $\pi \rightarrow \pi^*$ single excitations. This has been found adequate to determine the UV–visible absorption spectra provided that the suitable parameterizations are used. The CI method is widely employed in the calculation of absorption spectra. Using a CI method in combination with a semi-empirical model Hamiltonian, an evaluation of absorption spectra of large organic molecules, and LCs become possible. Hence, the author employed the CNDO/S–CI and INDO/S–CI methods including all valence electrons, and applied for the calculation of electronic spectra of the molecules. In the present computation, a comparative analysis has been carried out by employing the CNDO/S, INDO/S, and DFT methods to calculate the UV–vis absorption spectrum. The DFT calculations have been performed by a spectroscopy oriented configuration interaction procedure (SORCI) [25], however, a revised version of QCPE 174 by Jeff Reimers, University of Sydney, and coworkers have been used for the semiempirical calculations. The charge distributions of molecules have been calculated by performing Mulliken, and Loewdin population analysis.

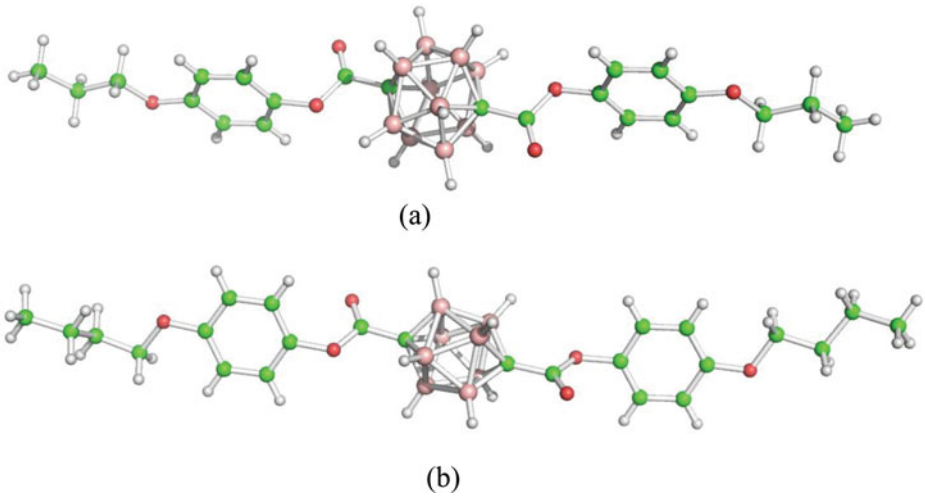

Figure 1. The molecular structures of (a) Nematic1 ($C_{22}H_{32}B_{10}O_6$) and (b) Nematic2 ($C_{24}H_{34}B_8O_6$) molecules.

Results and discussion

The electronic structures of Nematic1 and Nematic2 molecules have been shown in Fig. 1. The molecular charge distribution, phase stability, and optical properties of the molecules have been discussed below:

Charge distribution and phase stability

To parameterize the molecular level computational studies, partial charges are helpful. Quantum-chemical computations offer the possibility to take a detailed look at the electronic structure of the molecules. This can be done by determining atom-based partial charges.

The group charges are needed to explain the behavior of mesogens. In view of this, Mulliken population analysis that partitions the total charge among the atoms in the molecule, has been performed and the results have been compared with those obtained from Loewdin population analysis. Much agreement between the methods has been found in terms of the group charges of each molecule. Evidently (Table 1), the positively charged alkyl chains of Nematic1 will be strongly attracted by the negatively charged side group as well as the core, causing the formation of longer units in the nematic phase. Hence, the nematic phase stability is expected to be high for Nematic1. Further, the thermal vibration amplitude of the chain carbon atoms increase markedly with the increase of chain length, indicating a low packing efficiency for Nematic2. This leads to the drastic decrease in nematic phase stability. The present computations support to the N–I transition temperatures reported by the crystallographer (Table 1).

Table 1. Mulliken (M) and Loewdin (L) group charges and nematic–isotropic transition temperatures for Nematic1 and Nematic2 molecules.

	Side Group		Core		Alkyl		
Molecule	M	L	M	L	M	L	$T_{N\text{-}I}$/K [8]
Nematic1	− 0.39	− 0.34	− 0.25	− 0.18	0.63	0.52	468
Nematic2	− 0.40	− 0.35	− 0.21	− 0.17	0.61	0.52	456.4

Table 2. The vertical excited energy (E_V), and oscillator strength (f) of Nematic1, and Nematic2 molecules corresponding to absorption maxima (λ_{max}) at TDDFT, CNDO/S, and INDO/S levels.

Molecule	TDDFT	CNDO/S	INDO/S
	λ_{max}		
Nematic1	204.69	246.29	207.62
Nematic2	205.27	247.46	204.06
	EV		
Nematic1	6.06	5.02	5.97
Nematic2	6.04	5.00	5.98
	f		
Nematic1	0.11	0.74	0.12
Nematic2	0.14	0.75	0.15

UV–visible absorption spectrum

Increasing the number of carbon atoms in the end chain is the widely used technique to alter the physical properties of LC molecules. The description of molecular quantities by quantum-chemical methods underlies some principle restrictions [26], i.e., there exists a compromise between the complexity of the systems studied and the accessible theoretical accuracy. In the calculation of electronic spectra, the configuration interaction (CI) method is widely employed. Using a CI method in combination with a semi-empirical model Hamiltonian, an evaluation of absorption spectra of large organic molecules and LCs becomes possible. The principal absorption bands in the molecules are due to the $\pi \rightarrow \pi^*$ transitions in the core part (the cage like structure in this case) of the molecule. In general, transitions are roughly conserved in the novel systems studied, but they are influenced by the conjugation length, degree of conjugation, and the different substituents.

The present computations have been carried out on molecules viz., Nematic1, and Nematic2 to study their UV stability on the shift of absorption wavelength, and the corresponding spectral data. The variation in the absorption spectra has been observed due to the increment of carbon atoms in the end and side groups. The detailed analysis of absorption spectra of isolated molecules based on TDDFT calculations has been discussed below. However, the spectral data have been listed in Tables 2 and 3, respectively.

Nematic 1 and nematic 2

The absorption spectrum of Nematic1 is shown in Fig. 2 based on the DFT, CNDO/S, and INDO/S methods. The DFT data show that three strong absorptions at 204.69 nm (λ_1), 239.84 nm (λ_2), and 271.48 nm (λ_3) have been observed in the UV region. However, no absorption has been observed in the visible region. The strongest band appears in a region

Table 3. Calculated highest occupied molecular orbital (HOMO), the lowest unoccupied molecular orbital (LUMO) energies, and energy gap $E_g = E_{LUMO} - E_{HOMO}$, of compounds using TDDFT, CNDO/S, and INDO/S levels.

Molecule	Method	HOMO (eV)	LUMO (eV)	E_g (eV)
Nematic1	TDDFT	− 8.75	− 0.43	8.32
	CNDO/S	− 8.20	− 2.59	5.61
	INDO/S	− 8.23	− 0.60	7.63
Nematic2	TDDFT	− 8.67	− 0.61	8.06
	CNDO/S	− 8.56	− 2.37	6.19
	INDO/S	− 8.15	− 0.61	7.54

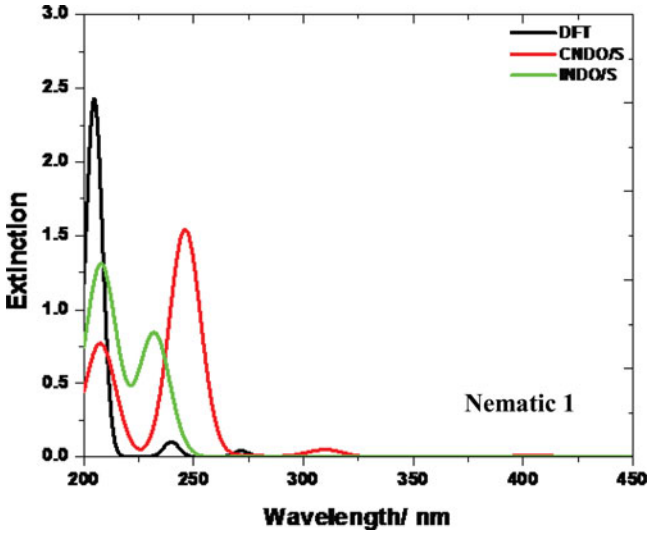

Figure 2. Absorption spectra of Nematic1 molecule using DFT, CNDO/S, and INDO/S approximations. Extinction unit: 10^4 dm^3 mol^{-1} cm^{-1}.

of 200–216.99 nm with absorption maxima (λ_{max}) at 204.69 nm (λ_3). This band arises from the HOMO→LUMO transition and is assigned as $\pi \rightarrow \pi^*$ transitions in the molecule. The observed oscillator strength (*f*) values corresponding to three wavelengths are 0.11, 0.09, and 0.03, respectively. Further, the calculation also predicts $\pi \rightarrow \pi^*$ transitions corresponding to weak absorption bands at the remaining two wavelengths (λ_2 and λ_3).

Figure 3 shows the absorption spectra of Nematic2 using the similar methods as discussed above. The DFT data show three prominent bands in the UV region with strong absorptions at 205.27 nm (λ_1), 242.77 nm (λ_2), and 273.24 nm (λ_3). The strongest band has been observed from 200 nm to 217.58 nm with absorption maxima at 205.27 nm. However, no absorption has been observed in the visible region. This band arises due to the HOMO→LUMO transition

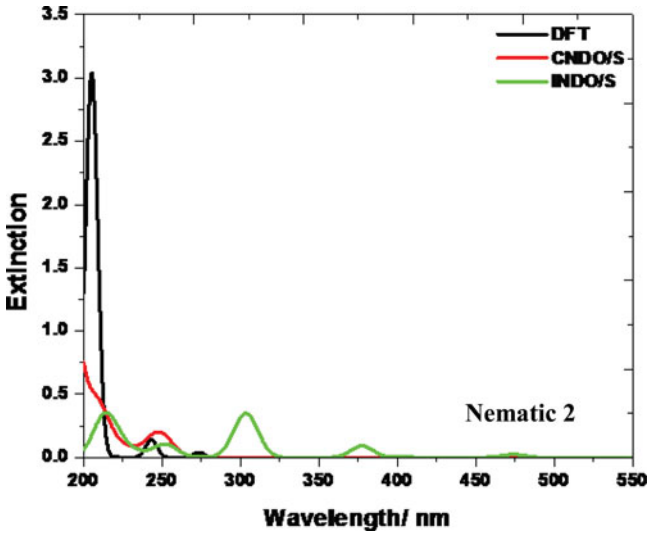

Figure 3. Absorption spectra of Nematic2 molecule using DFT, CNDO/S, and INDO/S approximations. Extinction unit: 10^4 dm^3 mol^{-1} cm^{-1}.

and is assigned as $\pi \rightarrow \pi^*$ transitions in the molecule. The oscillator strength (f) corresponding to λ_1, λ_2, and λ_3 are 0.14, 0.10, and 0.03, respectively. However, the appearance of weak absorption bands at λ_2 and λ_3 indicates the possibility of additional $\pi \rightarrow \pi^*$ transitions.

Thus, the substitution of additional alkyl group in Nematic1 on both sides (forming Nematic 2) leads to a bathochromic shift (the shift of absorption maxima to a longer wavelength). Further, increment in the alkyl chain length shows hyperchromic effect (increment in absorbance). The shift may be understood due to the ease in transfer of electrons through the conjugated system with increase in size as well as the planarity of molecules that results into the decrement of optical gap. Evidently, the DFT and

INDO/S methods show a good agreement in the shift of absorption wavelength. The tendency of absorption wavelength with respect to the substitution of additional alkyl group is the same in both methods. However, a deviation in shift of absorption maxima has been observed for both molecules using the CNDO/S method. A comparative picture of the vertical excited energy (E_V), and the oscillator strength (f) corresponding to absorption maxima (λ_{max}) using the CNDO/S, INDO/S, and TDDFT methods have been reported in Table 2. The lower chain length causes higher transition energy. In view of this, it may be understood that calculated vertical excitation energies are relatively sensitive to the method and the end chain length. Evidently, the electronic transitions among the methods reveal that the maximum oscillator strength is exhibited by Nematic2 molecule in UV range at longer wavelength side (Table 2). Further, the absorption maxima of Nematic2 are higher as per the DFT and CNDO/S data. However, a little deviation has been observed in case of INDO/S data. Hence, the UV stability and the flexibility for electronic transitions of Nematic 2 are higher that may be exploited for several optoelectronic applications.

The oscillator strength is a dimensionless quantity that expresses the probability of absorption of electromagnetic radiation in transitions between energy levels of an atom or molecule. It indicates the allowedness of electronic transitions in a molecule, and it is particularly valuable as a method of comparing "transition strengths" between different types of quantum-mechanical systems. A graph has been plotted between wavelength and oscillator strength (Fig. 4) to understand the intensity profiles of the molecules. It may be observed from the figure that Nematic1 exhibits the highest oscillator strength at 202.70 nm, while Nematic2

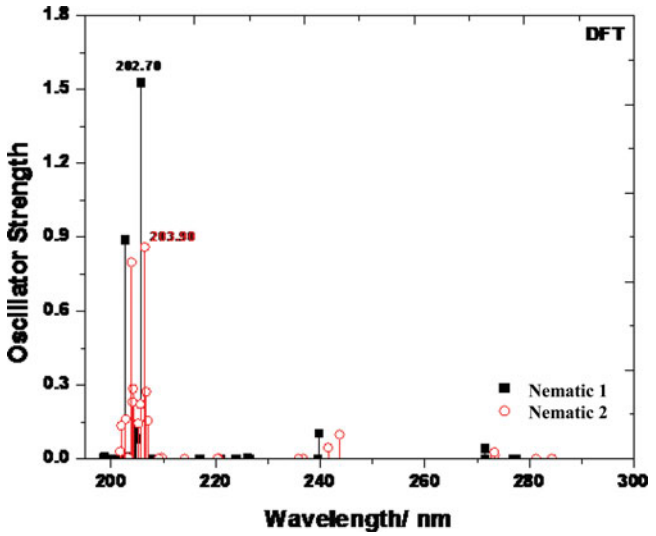

Figure 4. Intensity profiles of $C_{22}H_{32}B_{10}O_6$ and $C_{24}H_{34}B_8O_6$ molecules using DFT method.

at 203.90 nm. Further, these molecules exhibit the last intensity peak around 277.50 nm and 284.30 nm, respectively. This indicates the much flexibility of Nematic2 for electronic transitions over a long wavelength region, which causes high photosensitivity. The continuous decrease in absorption (Figs. 2 and 3), and oscillator strength (Fig. 4) clearly indicates the breakage of aromatic rings with respect to the higher wavelengths, and subsequently loosing the photosensitivity. This decrease in absorption as a function of increasing UV–visible wavelength has been consistently observed for both the molecules.

HOMO–LUMO analysis

The HOMO level can be thought the outermost orbital containing electrons, tends to give these electrons such as an electron donor. On the other hand, LUMO can be thought the innermost orbital containing free places to accept electrons. Owing to the interaction between HOMO and LUMO orbital of a structure, transition of state $\pi \rightarrow \pi^*$ type is observed with regard to the molecular orbital theory. Therefore, while the energy of the HOMO is directly related to the ionization energy, LUMO energy is directly related to the electron affinity. Energy difference between HOMO and LUMO orbital is called as energy gap, which is an important factor for analyzing the stability of the structures. The lowering of energy separation between the HOMO and LUMO clearly explicates the charge transfer interactions taking place within the molecule.

A comparison of HOMO, LUMO energies, and energy gap (E_g) values has been reported in Table 3. Evidently, the molecules exhibit much agreement between DFT and INDO/S methods. The HOMO value of Nematic2 is higher, due to the longer shift λ_{max} after substitution. However, the energy gap (E_g) shows a preference with increment in end alkyl groups. The increment of alkyl groups in the end chain causes a decrement in optical gap E_g, thereby increasing the conductivity of the molecule. Further, the Nematic2 molecule has a small energy band gap in comparison to Nematic1 molecule. Hence, this finding also confirms the high flexibility of Nematic2.

Since the energy gap determines the molecular reactivity such as the ability to absorb light, and to react with other species, a molecule with small gap (Nematic2 in this case) is expected to have higher reactivity and a lower stability in photo-physical processes.

Conclusions

The salient features of the present work are:

1. Nematic2 molecule shows the much flexibility for electronic transitions over a long wavelength region that leads to higher photosensitivity.
2. The HOMO value of Nematic2 is higher due to the longer shift λ_{max} after substitution.
3. The increment of alkyl groups in the end chain causes a decrement in optical gap E_g, thereby increasing the conductivity of the molecule. Further, the Nematic2 has a small energy band gap in comparison to Nematic1. Hence, this also supports to the flexibility of Nematic2.
4. Since the energy gap determines the molecular reactivity such as the ability to absorb light, and to react with other species, a molecule with small gap (i.e., Nematic2) is expected to have higher reactivity and lower stability in photo-physical processes.

Acknowledgments

The financial support provided by SERB-DST, and CSIR, New Delhi, India is gratefully acknowledged.

References

[1] Ojha, D. P. (2014). *Mol. Cryst. Liq. Cryst.*, *591*, 1–9.
[2] Praveen, P. L., & Ojha, D. P. (2012). *Mat. Chem. Phys.*, *135*, 628–634.
[3] Aneela, R., Praveen, P. L., & Ojha, D. P. (2012). *J. Mol. Liq.*, *166*, 70–75.
[4] Kaczmarczyk, A., & Kolski, G. B. (1964). *J. Phys. Chem.*, *68*, 1227–1229.
[5] Kaczmarczyk, A., & Kolski, G. B. (1965). *Inorg. Chem.*, *4*, 665–671.
[6] Ringstrand, B. (2013). *Liq. Cryst. Today*, *22*, 22–35.
[7] Nataraj, A., Balachandran, V., & Karthick, T. (2013). *J. Mol. Struct.*, *1038*, 134–144.
[8] Bene, J. D., & Jaffe, H. H. (1968). *J. Chem. Phys.*, *48*, 1807–1813.
[9] Bene, J. D., & Jaffe, H. H. (1968). *J. Chem. Phys.*, *48*, 4050–4055.
[10] Bene, J. D., & Jaffe, H. H. (1968). *J. Chem. Phys.*, *49*, 1221–1229.
[11] Bene, J. D., & Jaffe, H. H. (1968). *J. Chem. Phys.*, *50*, 1126–1129.
[12] Ellis, R. L., Kuehnlenz, G., & Jaffe, H. H. (1972). *Chim. Acta*, *26*, 131–140.
[13] Bacon, A. D., & Zerner, M. C. (1979). *Theor. Chim. Acta*, *53*, 21–54.
[14] Zerner, M. C., Loew, G. H., Kirchner, R. F., & Westerhoff, U. T. M. (1980). *J. Am. Chem. Soc.*, *102*, 589–599.
[15] Kaszynskia, P., Januszkoa, A., Ohtab, K., Nagamine, T., Potaczeka, P., Young Jr., V. G., & Endo, C. Y. (2008). *Liq. Cryst.*, *35*, 1169–1190.
[16] Stratmann, R. E., Scuseria, G. E., & Frisch, M. J. (1998). *J. Chem. Phys.*, *109*, 8218–8224.
[17] Neugebauer, A., & Hafelinge, G. (2002). *J. Mol. Struct. Theochem.*, *585*, 35–47.
[18] Cornaton, Y., Franck, O., Teale, A. M., & Fromager, E. (2013). *Mol. Phys.*, *111*, 1275–1294.
[19] Lee, C., Yang, W., & Parr, R. G. (1988). *Phys. Rev.*, *B37*, 785–789.
[20] Hohenberg, P., & Kohn, W. (1965). *Phys. Rev.*, *136*, B864–B871.
[21] Head, J. D., & Zerner, M. C. (1986). *Chem. Phys. Lett.*, *131*, 359–366.
[22] Edwalds, W. D., & Zerner, M. C. (1987). *Theor. Chim.Acta.*, *72*, 347–361.
[23] Kohn, W., & Sham, L. J. (1965). *Phys. Rev.*, *140*, A1133–A1188.
[24] Jones, R. O., & Gunnarsson, O. (1989). *Rev. Mod. Phys.*, *61*, 689–746.
[25] Neese, F. A. (2003). *J. Chem.Phys.*, *119*, 9428–9444.
[26] Targema, M., Egbdi, M. O. O., & Adeyoe, M. D. (2013). *Comp. Theor. Chem.*, *1012*, 47–53.